Cancer Science
Japanese Cancer Association JCA
Open Access

In vivo imaging of membrane type-1 matrix metalloproteinase with a novel activatable near-infrared fluorescence probe

Yoichi Shimizu,[1,2,4] Takashi Temma,[1,4] Isao Hara,[3] Akira Makino,[1] Naoya Kondo,[1] Ei-ichi Ozeki,[3] Masahiro Ono[1] and Hideo Saji[1]

[1]Department of Patho-Functional Bioanalysis, Graduate School of Pharmaceutical Sciences, Kyoto University, Kyoto; [2]Central Institute of Isotope Science, Hokkaido University, Sapporo; [3]Technology Research Laboratory, Shimadzu Corporation, Kyoto, Japan

Key words

Activatable probe, membrane type-1 matrix metalloproteinase, molecular imaging, near-infrared, optical

Correspondence

Hideo Saji, Department of Patho-Functional Bioanalysis, Graduate School of Pharmaceutical Sciences, Kyoto University, 46-29 Yoshida Shimoadachi-cho, Sakyo-ku, Kyoto 606-8501, Japan.
Tel: +81-75-753-4556; Fax: +81-75-753-4568;
E-mail: hsaji@pharm.kyoto-u.ac.jp

[4]These authors contributed equally to this work.

Funding information

This study was supported in part by MEXT KAKENHI Grant Number 23113509. Part of this study was supported by the New Energy and Industrial Technology Development Organization, Japan.

Received November 25, 2013; Revised May 20, 2014; Accepted May 22, 2014

Cancer Sci **105** (2014) 1056–1062

doi: 10.1111/cas.12457

Membrane type-1 matrix metalloproteinase (MT1-MMP) is a protease activating MMP-2 that mediates cleavage of extracellular matrix components and plays pivotal roles in tumor migration, invasion and metastasis. Because *in vivo* noninvasive imaging of MT1-MMP would be useful for tumor diagnosis, we developed a novel near-infrared (NIR) fluorescence probe that can be activated following interaction with MT1-MMP *in vivo*. MT1-hIC7L is an activatable fluorescence probe comprised of anti-MT1-MMP monoclonal antibodies conjugated to self-assembling polymer micelles that encapsulate NIR dyes (IC7-1, λ_{em}: 858 nm) at concentrations sufficient to cause fluorescence self-quenching. In aqueous buffer, MT1-hIC7L fluorescence was suppressed to background levels and increased approximately 35.5-fold in the presence of detergent. Cellular uptake experiments revealed that in MT1-MMP positive C6 glioma cells, MT1-hIC7L showed significantly higher fluorescence that increased with time as compared to hIC7L, a negative control probe lacking the anti-MT1-MMP monoclonal antibody. In MT1-MMP negative MCF-7 breast adenocarcinoma cells, both MT1-hIC7L and hIC7L showed no obvious fluorescence. In addition, the fluorescence intensity of C6 cells treated with MT1-hIC7L was suppressed by pre-treatment with an MT1-MMP endocytosis inhibitor ($P < 0.05$). *In vivo* optical imaging using probes intravenously administered to tumor-bearing mice showed that MT1-hIC7L specifically visualized C6 tumors (tumor-to-background ratios: 3.8 ± 0.3 [MT1-hIC7L] *vs* 3.1 ± 0.2 [hIC7L] 48 h after administration, $P < 0.05$), while the probes showed similarly low fluorescence in MCF-7 tumors. Together, these results show that MT1-hIC7L would be a potential activatable NIR probe for specifically detecting MT1-MMP-expressing tumors.

Cancer is among the diseases with the highest morbidity and mortality rates worldwide, and a variety of basic and clinical work has been performed to seek effective treatments for various cancer types. To achieve effective qualitative diagnoses, detection of biomolecules related to tumor malignancy is highly important.[1]

Matrix metalloproteinases (MMP) are zinc endopeptidases with 16 secreted MMP and seven membrane-associated MMP (MT-MMP) identified to date. MMP play key roles in tissue remodeling, organ development and wound healing.[2,3] Among MMP family members, membrane type-1 MMP (MT1-MMP, also called MMP-14) is known to be expressed on the surface of tumor cells during the early stages of several cancers[4] and has a pivotal role in tumor migration and metastasis by participating in the remodeling of the extracellular matrix and transmitting survival signals[5–7] that could accelerate tumor malignancy in a wide variety of cancers. Furthermore, MT1-MMP was recently reported to induce tumor-initiating cell invasion under hypoxic conditions and, thereby, control metastasis,[8] and MT1-MMP overexpression was found to induce epithelial-to-mesenchymal transition, which is known to be associated with tumor progression and generation of cancer stem cells.[9] Therefore, MT1-MMP holds great promise as an early biomarker for the diagnosis of malignant tumors.

Several imaging modalities such as PET and MRI have been developed and used clinically. Among these, optical imaging systems can offer convenient and safe images, having pronounced spatial and temporal resolution, which are desirable for *in vivo* applications in clinical and basic research.

Previously, we produced a self-quenching activatable fluorescence probe "anti-MT1-MMP mAb-ROX, (MT1-ROX)," and confirmed that the cellular internalization of MT1-MMP activated MT1-ROX fluorescence, which allowed the visualization of MT1-MMP expression in tumor cells.[10] However, MT1-ROX emits fluorescence in the visible region (λ_{ex} = 575 nm, λ_{em} = 602 nm), which precludes its use in *in vivo* imaging. In contrast, we previously developed a novel fluorescence probe "IC7L," a self-assembling polydepsipeptide

polymer micelle "lactosome" that encapsulates the cyanine dye "IC7-1", which has fluorescence signals in the near-infrared (NIR) region (700–1000 nm); this is optimal for *in vivo* imaging due to the minimal light absorption, scatter and autofluorescence in this region.[11] Furthermore, we found that IC7L encapsulating high concentrations of hydrophobic polymer (poly-L-lactate) conjugated IC7-1 (hIC7L) showed stable fluorescence quenching to background levels in aqueous solution and plasma, and fluorescence dequenching following micelle denaturation accompanied by cellular internalization of hIC7L.[12] Based on these findings, we planned to apply hIC7L to design an MT1-MMP imaging probe that would allow *in vivo* visualization of MT1-MMP in tumors.

In this study, we first prepared MT1-hIC7L composed of hIC7L and an anti-MT1-MMP monoclonal antibody. We expected that the quenched MT1-hIC7L would first recognize MT1-MMP expressed on the surface of target tumor cells, and then be delivered into the cell following internalization of MT1-MMP, whereupon probe denaturation or metabolism would result in dequenching of the encapsulated dye and subsequent dye fluorescence (Fig. 1). Therefore, we evaluated the effectiveness of the activatable system in MT1-MMP-expressing tumors and the potential of MT1-hIC7L as a specific imaging probe for MT1-MMP-expressing tumors using *in vitro* cellular uptake assays and *in vivo* imaging studies.

Materials and Methods

Preparation of MT1-hIC7L. All chemicals were commercially available and of the highest purity. The amphiphilic polymer block of the lactosome, poly(sarcosine)-b-poly(L-lactic acid) block copolymer with 70 and 30 average degrees of polymerization on the former and latter blocks, respectively, with glycol capping at the *N*-terminus ($PSar_{70}$-block-$PLLA_{30}$), was supplied by the Shimadzu Corporation (Kyoto, Japan).

Maleimide group-coupled hIC7L (maleimide-hIC7L) was prepared as previously described. In brief, the poly(sarcosine)-b-poly(L-lactic acid) block copolymer with 75 and 30 average degrees of polymerization for the respective former and latter blocks and a maleimide group coupled to the *N*-terminus of the lactosome (maleimide-$PSar_{75}$-block-$PLLA_{30}$) (194 nmol), $PSar_{70}$-block-$PLLA_{30}$ (194 nmol), and IC7-1-$PLLA_{30}$ (97 nmol) dissolved in chloroform (500 μL) were dripped into a glass test tube. The solvent was removed under reduced pressure to form a thin film on the tube wall. PBS (0.1 M, pH 7.4) was then added to the test tube and heated at 82°C for 20 min. The resulting aqueous solution was filtered through a 0.20-μm Acrodisc syringe filter (Pall Corp, East Hills, NY, USA) to yield maleimide-hIC7L.

Anti-MT1-MMP antibody was prepared as shown previously by hybridoma methods with the epitope sequence between 295Pro and 311Asn at the hinge region of the MT1-MMP protein.[13] The specific reactivity of this antibody to MT1-MMP was analyzed using western blotting, as described in the supporting materials and shown in Fig. S1. The anti-MT1-MMP antibody (2.5 mg/mL 0.16 M borate buffer, pH 8.0) was reacted with 2-iminothiolane (10 mg/mL 0.16 M borate buffer, pH 8.0) for 1 h on ice. The reactant was deoxidized by reaction with dithiothreitol (0.3 mg/2 μL) for 15 min and then purified on a Sephadex G-50 column. The resulting anti-MT1-MMP antibody with the thiol group was added to the maleimide-hIC7L and incubated for 4 h on ice with protection from light. After incubation, cysteine·HCl (158 μg) was added to the reactant and incubated for a further 30 min. The mixture was then purified on a Superdex 200 10/300 GL column (GE Healthcare Japan Corporation, Tokyo, Japan) equilibrated with PBS(−) at a flow rate of 0.5 mL/min. The high molecular weight fraction (retention time: 14–16 min) was collected to obtain MT1-hIC7L. The size distribution of MT1-hIC7L was measured at 25°C using a Zetasizer Nano-S90 (Malvern Instruments Ltd, Malvern, UK). The concentration of the anti-MT1-MMP antibody conjugated to MT1-hIC7L was measured using a bicinchoninic acid (BCA) assay, and the number (molar ratio) of anti-MT1-MMP antibodies per hIC7L was calculated using estimated molecular weight values of 150 and 1315 kDa for the anti-MT1-MMP antibody and hIC7L, respectively. The purity was analyzed by size exclusion chromatography using a Superdex 200 10/300 GL column (GE Healthcare) equilibrated

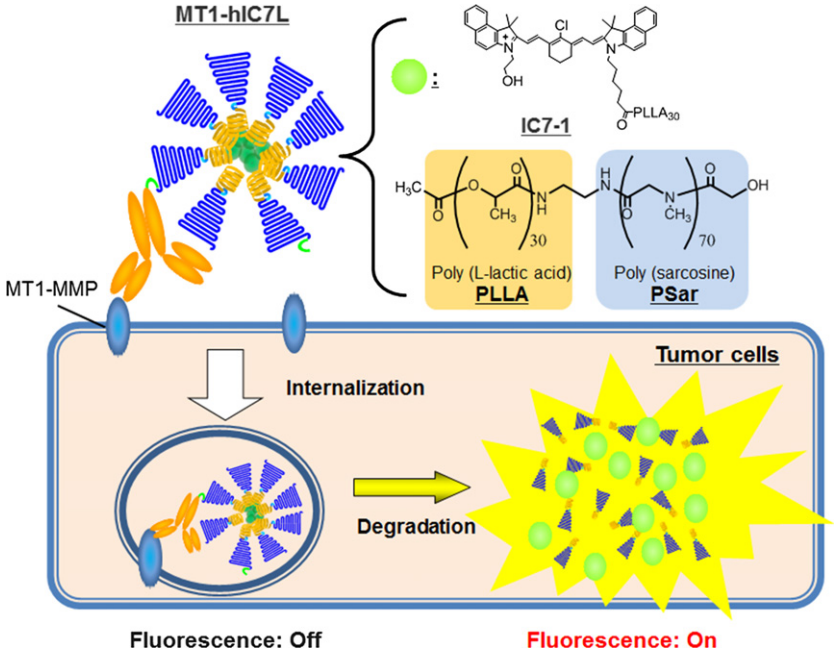

Fig. 1. Schematic illustration of the design and strategy of MT1-hIC7L. Quenched MT1-hIC7L first attaches to membrane type-1 matrix metalloproteinase (MT1-MMP) expressed on tumor cells, and is then delivered to the cell interior via MT1-MMP internalization whereupon fluorescence signals are emitted following probe degradation.

with PBS at a flow rate of 0.5 mL/min. Absorbance at 215 and 830 nm was used to detect the lactosome and IC7-1, respectively, which confirmed that the absorbance peaks at both wavelengths were detected simultaneously in the high molecular weight fraction. The affinity of MT1-hIC7L for MT1-MMP was evaluated by flow cytometry using methods similar to those described previously (Data S1 and Fig. S2).[14]

Optical properties of MT1-hIC7L. MT1-hIC7L (1 mg/mL, 100 μL) was incubated in 100 μL PBS (0.1 M, pH 7.4) with or without SDS (5% final concentration) for 30 min at room temperature. After incubation, 0.8 mL PBS was added to the solution and fluorescence images were acquired using a Clairvivo OPT (Shimadzu Corporation) with a 785-nm laser diode for excitation and a 845/55-nm band path filter for emission. The fluorescence emission spectra were also measured with a fluorescence spectrometer (Fluorolog-3; HORIBA Jobin Yvon Inc, Kyoto, Japan) following excitation at 815 nm using a slit width of 5 nm for both excitation and emission measurements.

Cellular uptake study. C6 glioma cells (HSRRB, Tokyo, Japan) (MT1-MMP high-expressing tumor cells) and MCF-7 human breast adenocarcinoma cells (ATCC, Manassas, VA, USA) (MT1-MMP low-expressing cells) were cultured in DMEM medium with 10% FBS at 37°C in a humidified atmosphere containing 5% CO_2.[10] After pre-incubation of cells (2×10^5 cells) overnight in 24-well poly-D-lysine-coated dishes (Biocoat, Becton Dickinson, San Jose, CA, USA), probes (40 μg/1 mL DMEM with 50 μM BSA) were added and incubated at 37°C in a humidified atmosphere containing 5% CO_2. At 30 min, 1, 3 and 6 h, the cells were washed twice with PBS and fluorescence images were acquired using a Clairvivo OPT with a 785 nm laser diode for excitation and a 845/55 nm band path filter for emission. After image acquisition, the cells were treated with 0.2 N NaOH and the cell lysate protein concentrations were measured by BCA assay. The fluorescence intensity of the cells was analyzed using Clairvivo OPT display software version 2.60. The fluorescence intensity of the cells was represented as a ratio to the dosage as follows:

$$\text{FI Ratio} = \frac{[\text{Fluorescence Intensity of the cells}]}{[\text{Fluorescence Intensity of the probe added to the cells}] \times [\text{Cell lysate (mg protein)}]}$$

For the blocking study, C6 cells were treated with type I collagen (Col I; 100 μg/1 mL DMEM) for 24 h at 37°C. The cells were washed twice with PBS, and then MT1-hIC7L (40 μg/1 mL DMEM with 50 μM BSA) was added. After incubation for 30 min, 1, 3 and 6 h, cells were washed twice with PBS. Subsequent fluorescence measurements were carried out as described above.

Preparation of tumor bearing mice. Female nude mice (BALB/c nu/nu) and female SHO mice (SHO-*Prkdc*^{scid}*Hr*^{hr}) supplied by Japan SLC Inc (Hamamatsu, Japan) and Charles River Laboratories Japan (Yokohama, Japan) respectively, were housed under a light : dark 12:12 h cycle and given free access to food and water. The animal experiments performed in the present study were conducted in accordance with institutional guidelines and approved by the Kyoto University Animal Care Committee, Japan. C6 cells (5×10^6 cells in 100 μL) were subcutaneously inoculated into the right hind legs of 4-week-old female nude mice (BALB/c nu/nu), and an *in vivo* imaging study was performed after a 2-week growth period. For preparation of MCF-7 xenografted mice, 5-week-old female SHO mice were first implanted subcutaneously with a 0.72-mg 60-day release 17-estradiol pellet (Innovative Research of America, Toledo, OH, USA). The next day, MCF-7 cells (1.0×10^7 cells) suspended in 100 μL PBS containing 50% Geltrex were subcutaneously inoculated into the left hind legs. Six weeks after transplantation, the MCF-7 tumor-bearing mice were used for the following imaging study. The MT1-MMP expression levels in C6 and MCF-7 xenografted tumors were also evaluated by western blotting and immunohistochemical methods, as described in Data S1, and the results are shown in Fig. S3.

***In vivo* imaging study.** MT1-hIC7L or hIC7L (2 mg/mL PBS, 100 μL) were injected into tumor-bearing mice through the tail vein and NIR fluorescence images were collected using a Clairvivo OPT with a 785-nm laser diode for excitation, and a 845/55-nm band path filter for emission. During the imaging process, mice remained on the imaging stage under anesthesia using 2.5% isoflurane gas in oxygen (1.5 L/min). Regions of interest (ROI) were designated for the tumor and background (around the neck) on the acquired images to measure fluorescence intensities.

Statistics. Data are represented as the mean ± SD. Statistical analyses were performed with two-way factorial ANOVA followed by a Tukey–Kramer test. A two-tailed value of $P < 0.05$ was considered to be statistically significant.

Results

Probe preparation and determination of optical properties. The particle sizes of MT1-hIC7L and hIC7L were 44.9 ± 1.7 nm ($n = 3$) and 35.1 ± 0.4 nm ($n = 3$), respectively. The presumed average molar ratio of anti-MT1-MMP antibody conjugated to hIC7L was 1.4 ± 0.1 ($n = 3$). The immunoreactivity of MT1-hIC7L relative to MT1-MMP as measured by flow cytometry was slightly decreased compared to the anti-MT1-MMP antibody but was higher than for the control groups treated with only PBS (Fig. S2).

MT1-hIC7L fluorescence was suppressed to background levels in aqueous buffer (PBS), and increased in SDS solution (Fig. 2a). The fluorescence intensity was also quantified from the images and the ratio of the intensity in SDS solution compared to that in PBS was 35.5 ± 6.2. The fluorescence spectrum of MT1-hIC7L was also apparent in SDS solution but not in PBS (Fig. 2b).

***In vitro* study.** MT1-hIC7L fluorescence in C6 cells, which have high MT1-MMP expression levels, increased gradually and was significantly higher than that of hIC7L 3 h or more after addition (Fig. 3a). In contrast, probe uptake by MCF-7 cells (low MT1-MMP expression levels) was consistently low for both probes (Fig. 3b). When cells were pretreated with the endocytosis inhibitor Col I, the fluorescence intensity of cells incubated with MT1-hIC7L was significantly depressed compared to that of the non-pretreated group (Fig. 3c).

***In vivo* imaging study.** Compared to the hIC7L administered group, in MT1-hIC7L administered mice the fluorescence gradually increased in C6 xenografted tumors, which could be imaged clearly at 24 and 48 h post-administration (Fig. 4a). In addition, the T/B ratios of MT1-hIC7L increased with time and provided higher values than those of hIC7L (Fig. 4c, 3.2 ± 0.3 *vs* 2.7 ± 0.2 at 24 h, and 3.8 ± 0.3 *vs* 3.1 ± 0.2 at 48 h). In mice xenografted with MCF-7 cells which express low levels of MT1-MMP, there was no significant difference in the images between the MT1-hIC7L-administered and hIC7L-administered groups throughout the study duration (Fig. 4b). The T/B ratios in the MCF-7 tumors were

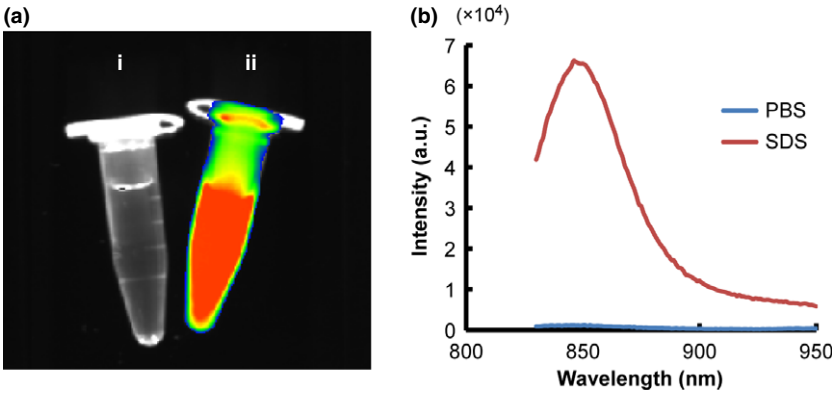

Fig. 2. Optical characteristics of activatable type IC7-1 lactosomes. (a) Fluorescence images of MT1-hIC7L after incubation in PBS buffer (i) or 5% SDS solution (ii) for 30 min. (b) Fluorescence emission spectrum of MT1-hIC7L after incubation in PBS buffer (blue) or 5% SDS solution (red) for 30 min.

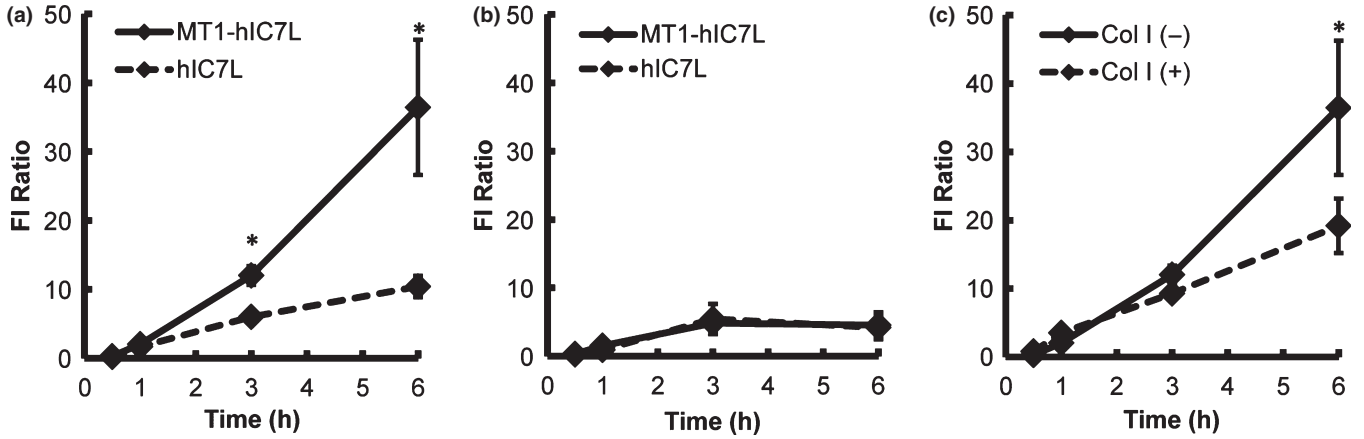

Fig. 3. Cell uptake of MT1-hIC7L. (a,b) C6 (a) or MCF-7 cells (b) were treated with MT1-hIC7L or hIC7L and the fluorescence intensities were acquired for 6 h. Data are expressed as the FI ratio (mean ± SD) for 4 samples. Comparison between the MT1-hIC7L- and hIC7L-treated groups was performed with two-way factorial ANOVA followed by Tukey–Kramer test (*$P < 0.01$ *vs* hIC7L). (c) The mean fluorescence intensity of C6 cells treated with (dotted line) or without Col I (solid line) for 6 h at 0.5, 1, 3 and 6 h after incubation with MT1-hIC7L. Data are expressed as%Intensity/mg protein (mean ± SD) for 4 samples. Comparisons between the Col I-treated (Col I [+]) and Col I-untreated groups (Col I [−]) were performed with two-way factorial ANOVA followed by the Tukey–Kramer test (*$P < 0.05$ *vs* Col I [+]).

unchanged regardless of the probe used (Fig. 4d, 2.5 ± 0.3 *vs* 2.6 ± 0.2 at 24 h, and 2.8 ± 0.4 *vs* 3.0 ± 0.2 at 48 h).

Discussion

In the present study, we developed MT1-hIC7L as an optical activatable probe for MT1-MMP detection. MT1-hIC7L fluorescence was effectively quenched in aqueous buffer, and then dramatically activated under micelle-degenerating conditions (Fig. 2) and in cells expressing high levels of MT1-MMP following MT1-MMP-dependent internalization (Fig. 3). In addition, high fluorescence levels were observed in MT1-MMP-expressing tumors in xenografted mice 24 and 48 h after MT1-hIC7L administration (Fig. 4).

In the cell uptake study, MT1-hIC7L showed fluorescence increasing with time only in C6 cells but continuously low fluorescence in MCF7 cells. The similar result obtained in another cell line that expresses high levels of MT1-MMP (HT1080 human fibroblastoma cells [Fig. S4]) coupled with the lack of significant hIC7L fluorescence regardless of the cells used, suggests that MT1-hIC7L dequenching was successfully achieved following specific interactions with MT1-MMP. Furthermore, we performed an inhibition study with Col I, an inhibitor of dynamin-dependent MT1-MMP internalization,[15] and found that the C6 cell fluorescence of the MT1-hIC7L-treated group was significantly decreased by Col I pre-treatment. The moderate fluorescence that was observed in the Col I pre-treated MT1-hIC7L group might be due to other MT1-MMP internalization processes, such as clathrin-independent mechanisms involving caveolae.[6,16] Nonetheless, the results indicate that the fluorescence activation of MT1-hIC7L in the MT1-MMP high expressing tumor cells was primarily dependent on MT1-MMP internalization.

In the *in vivo* study, significantly higher fluorescence was observed in C6 tumors in mice after MT1-hIC7L administration as compared with other groups. However, it should be noted that measurable fluorescence was observed in tumors of the hIC7L-administered groups, which was similar to our previous study with the fluorescent lactosome probe "IC7L" (T/B ratios for IC7L: 2.6 ± 0.4 at 24 h, and 3.1 ± 0.3 at 48 h).[11] Therefore, considering that quenched hIC7L still had weak fluorescence that was gradually dequenched in blood while still retaining its micelle structure,[12] the tumor fluorescence in hIC7L administered groups might reflect the lactosome biodistribution. In contrast, we previously reported that targeting ligands such as antibodies conjugated on the surface of lactosome would have negligible effects on the amount of lactosome probe delivered to tumor tissues because lactosomes are originally delivered to tumors at high levels by enhanced permeability and retention (EPR) effect, and this would lead to

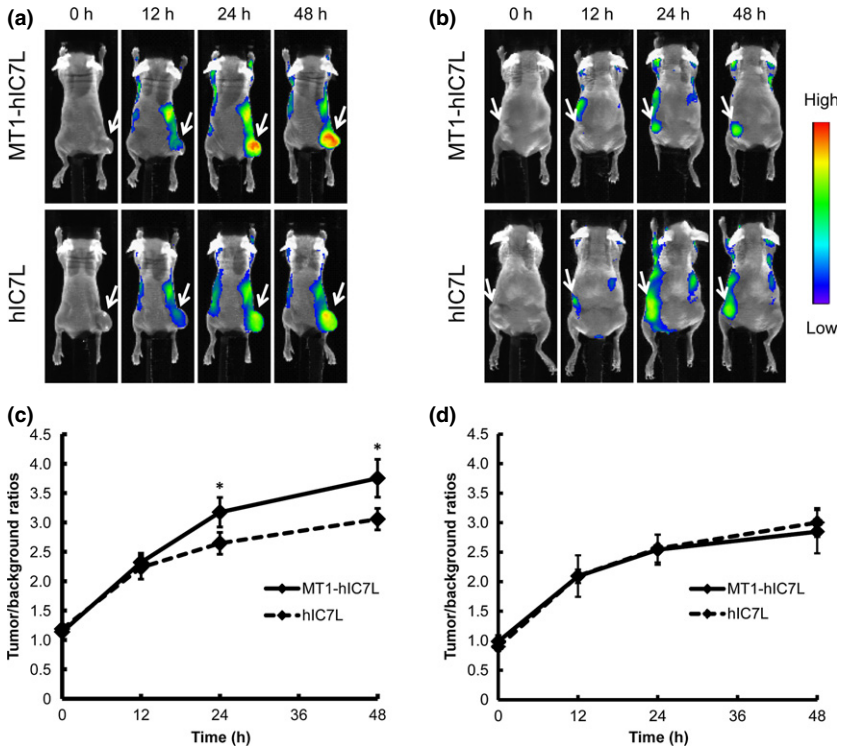

Fig. 4. *In vivo* imaging of MT1-hIC7L. (a,c) Fluorescence images of C6 cell xenografted mice (a) or MCF-7 xenografted mice (c) at 0 h (just after injection), 12, 24 and 48 h after administration of MT1-hIC7L (upper) and hIC7L (lower). Arrows indicate the tumor tissue. (b,d) The C6 tumor (b) or MCF-7 tumor (d) -to-background (T/B) fluorescence intensity ratios obtained from the region of interest of the tumor and background (neck) of mice administered MT1-hIC7L and hIC7L. Data are expressed as T/B ratio (mean ± SD). Comparison of the T/B ratios of MT1-hIC7L- and hIC7L-administered groups was performed with two-way factorial ANOVA followed by the Tukey–Kramer test (*$P < 0.05$ *vs* hIC7L).

difficulties in target biomolecule-specific *in vivo* imaging.[12] Therefore, in this study MT1-hIC7L could achieve MT1-MMP-specific *in vivo* imaging due to the combination of the fluorescence activatable hIC7L system and active targeting delivery system with the anti-MT1-MMP antibody, which enables probe internalization.

While MT1-hIC7L could visualize MT1-MMP-expressing tumors both *in vitro* and *in vivo*, non-specific fluorescence accumulation was observed in tumors of hIC7L-treated mice. Because nanocarriers with neutral or positive surface charges are known to cause non-specific cell internalization, as was reported in *in vitro* studies,[17,18] the surface charge of MT1-hIC7L (estimated to be −0.5 mV) might not be sufficiently negative to avoid non-specific cellular uptake in tumors, especially during the delayed phase after administration. In addition, the non-specific dequenching of hIC7L in the blood or tumor tissue might occur because of the relatively low probe stability in the blood. To address these issues, we are now trying to improve the probe presented in this study by modifying the hydrophilic moiety of the block polymer to modulate the surface charge, and by conjugating a D-lactate polymer to the NIR fluorophore to form a stereocomplex that is known to slow the degradation rate of the micelle complex due to its higher crystallinity.[19]

In this study, we chose the "lactosome" to be the optical probe core because of its suitable biodistribution, bioavailability and structure that allows for control of the resulting optical signals. Lactosomes have a favorable size (diameter: 30–40 nm) for delivery to tumor tissue through the EPR effect,[20] and can escape the reticuloendothelial system that can cause nonspecific accumulation of the probes in the abdominal region.[21] In addition, due to the composition of the biodegradable substances poly-sarcosine and poly-L-lactic acid, lactosomes have low toxicity, which is a point of concern for inorganic compounds such as quantum dots[22] and gold nanorods.[23–25] Furthermore, lactosomes have narrow hydrophobic cores in which lipophilic dyes may be encapsulated to high concentrations, which allows the formation of self-quenching states without affecting other probe qualities such as biodistribution. Compared with other fluorescence activatable systems such as photoinduced electron transfer (PeT) and Förster resonance energy transfer (FRET), self-quenching is preferable for its optical wavelength ranges around 800–900 nm where controlling optical signal can be difficult with PeT and FRET systems.[26,27] Therefore, the lactosome probe with its self-quenching activatable system appears to be a promising tool for noninvasive *in vivo* diagnostic techniques.

Several MT1-MMP dependent activatable optical probes that rely on the enzymatic activity of MT1-MMP and use the FRET system have been reported.[28,29] Whereas MT1-MMP internalization has been reported to play an important role in tumor cell migration and invasion,[6,16,30] there are no reports on probes that enable *in vivo* visualization of MT1-MMP internalization. Therefore, MT1-hIC7L activated by MT1-MMP internalization would provide additional valuable information for elucidating MT1-MMP functions in tumors. Furthermore, multicolor *in vivo* optical imaging is also emerging as a promising technique and can detect a variety of functions simultaneously.[31] The MT1-hIC7L fluorophore is IC7-1, which has absorption and emission wavelengths at 800–900 nm that are suitable for *in vivo* optical imaging, and offers fluorescence characteristics that differ significantly from commercially available or reported optical probes.[32] Therefore, we expect that the multicolor *in vivo* imaging with MT1-hIC7L and other reported FRET-type MT1-MMP imaging probes would offer further information to better understand the complicated role and relationship of MT1-MMP internalization with its enzyme activity in tumor tissue.

From a clinical standpoint, optical imaging technology has been rapidly advancing in terms of molecular probes as well as imaging modalities such as endoscopic cameras[26] and clinical breast scanners,[33] and is expected to provide an

informative navigation aid for surgical techniques.[34] In such image-guided surgery, NIR probes would be desirable due to their ability to discriminate between structures that are to be resected (e.g. tumor tissue) and spared (e.g. vessels or lymph node). Because NIR fluorescence can strongly penetrate through biological tissue, NIR-based probes would be useful for locating embedded structures.[35] As such, MT1-hIC7L would also be a clinically powerful tool for the diagnosis of tumor malignancy by specifically detecting MT1-MMP.

In summary, we developed MT1-hIC7L, which shows self-quenched fluorescence and specifically interacts with MT1-MMP expressed on tumor cells that internalize the probe, allowing the fluorescence to be dequenched after lactosome degeneration. These results indicate that MT1-hIC7L would be a useful NIR probe for specific imaging of MT1-MMP-expressing tumors.

Acknowledgments

This study was supported in part by MEXT KAKENHI Grant Number 23113509. Part of this study was supported by the New Energy and Industrial Technology Development Organization, Japan. Some experiments were performed at the Kyoto University Radioisotope Research Center.

Disclosure Statement

The authors have no conflict of interest to declare.

References

1 Liotta LA, Tryggvason K, Garbisa S, Hart I, Foltz CM, Shafie S. Metastatic potential correlates with enzymatic degradation of basement membrane collagen. *Nature* 1980; **284**: 67–8.
2 Deryugina EI, Quigley JP. Matrix metalloproteinases and tumor metastasis. *Cancer Metastasis Rev* 2006; **25**: 9–34.
3 Egeblad M, Werb Z. New functions for the matrix metalloproteinases in cancer progression. *Nat Rev Cancer* 2002; **2**: 161–74.
4 Sato H, Takino T, Okada Y *et al.* A matrix metalloproteinase expressed on the surface of invasive tumour cells. *Nature* 1994; **370**: 61–5.
5 Chen PS, Zhai WR, Zhou XM *et al.* Effects of hypoxia, hyperoxia on the regulation of expression and activity of matrix metalloproteinase-2 in hepatic stellate cells. *World J Gastroenterol* 2001; **7**: 647–51.
6 Uekita T, Itoh Y, Yana I, Ohno H, Seiki M. Cytoplasmic tail-dependent internalization of membrane-type 1 matrix metalloproteinase is important for its invasion-promoting activity. *J Cell Biol* 2001; **155**: 1345–56.
7 D'Alessio S, Ferrari G, Cinnante K *et al.* Tissue inhibitor of metalloproteinases-2 binding to membrane-type 1 matrix metalloproteinase induces MAPK activation and cell growth by a non-proteolytic mechanism. *J Biol Chem* 2008; **283**: 87–99.
8 Li J, Zucker S, Pulkoski-Gross A *et al.* Conversion of stationary to invasive tumor initiating cells (TICs): role of hypoxia in membrane type 1-matrix metalloproteinase (MT1-MMP) trafficking. *PLoS ONE* 2012; **7**: e38403.
9 Yang CC, Zhu LF, Xu XH, Ning TY, Ye JH, Liu LK. Membrane Type 1 Matrix Metalloproteinase induces an epithelial to mesenchymal transition and cancer stem cell-like properties in SCC9 cells. *BMC Cancer* 2013; **13**: 171.
10 Shimizu Y, Temma T, Sano K, Ono M, Saji H. Development of membrane type-1 matrix metalloproteinase-specific activatable fluorescent probe for malignant tumor detection. *Cancer Sci* 2011; **102**: 1897–903.
11 Shimizu Y, Temma T, Hara I *et al.* Development of novel nanocarrier-based near-infrared optical probes for *in vivo* tumor imaging. *J Fluoresc* 2012; **22**: 719–27.
12 Shimizu Y, Temma T, Hara I *et al.* Micelle-based activatable probe for *in vivo* near-infrared optical imaging of cancer biomolecules. *Nanomedicine* 2014; **10**: 187–95.
13 Kondo N, Temma T, Shimizu Y *et al.* Miniaturized antibodies for imaging membrane type-1 matrix metalloproteinase in cancers. *Cancer Sci* 2013; **104**: 495–501.
14 Temma T, Sano K, Kuge Y *et al.* Development of a radiolabeled probe for detecting membrane type-1 matrix metalloproteinase on malignant tumors. *Biol Pharm Bull* 2009; **32**: 1272–7.
15 Lafleur MA, Mercuri FA, Ruangpanit N, Seiki M, Sato H, Thompson EW. Type I collagen abrogates the clathrin-mediated internalization of membrane type 1 matrix metalloproteinase (MT1-MMP) via the MT1-MMP hemopexin domain. *J Biol Chem* 2006; **281**: 6826–40.
16 Galvez BG, Matias-Roman S, Yanez-Mo M, Vicente-Manzanares M, Sanchez-Madrid F, Arroyo AG. Caveolae are a novel pathway for membrane-type 1 matrix metalloproteinase traffic in human endothelial cells. *Mol Biol Cell* 2004; **15**: 678–87.
17 Yamamoto Y, Nagasaki Y, Kato Y, Sugiyama Y, Kataoka K. Long-circulating poly(ethylene glycol)-poly(D, L-lactide) block copolymer micelles with modulated surface charge. *J Control Release* 2001; **77**: 27–38.
18 Xiao K, Li Y, Luo J *et al.* The effect of surface charge on *in vivo* biodistribution of PEG-oligocholic acid based micellar nanoparticles. *Biomaterials* 2011; **32**: 3435–46.
19 Bertin A. Emergence of polymer stereocomplexes for biomedical applications. *Macromol Chem Phys* 2012; **213**: 2329–52.
20 Matsumura Y, Maeda H. A new concept for macromolecular therapeutics in cancer chemotherapy: mechanism of tumoritropic accumulation of proteins and the antitumor agent smancs. *Cancer Res* 1986; **46**: 6387–92.
21 Senior JH. Fate and behavior of liposomes *in vivo*: a review of controlling factors. *Crit Rev Ther Drug Carrier Syst* 1987; **3**: 123–93.
22 Derfus AM, Chan CWC, Bhatia SN. Probing the cytotoxicity of semiconductor quantum dots. *Nano Lett* 2004; **4**: 11–8.
23 Athanasiou KA, Niederauer GG, Agrawal CM. Sterilization, toxicity, biocompatibility and clinical applications of polylactic acid/polyglycolic acid copolymers. *Biomaterials* 1996; **17**: 93–102.
24 Tsai G, Lane HY, Yang P, Chong MY, Lange N. Glycine transporter I inhibitor, N-methylglycine (sarcosine), added to antipsychotics for the treatment of schizophrenia. *Biol Psychiatry* 2004; **55**: 452–6.
25 Murphy CJ, Gole AM, Stone JW *et al.* Gold nanoparticles in biology: beyond toxicity to cellular imaging. *Acc Chem Res* 2008; **41**: 1721–30.
26 Kobayashi H, Ogawa M, Alford R, Choyke PL, Urano Y. New strategies for fluorescent probe design in medical diagnostic imaging. *Chem Rev* 2010; **110**: 2620–40.
27 Luo S, Zhang E, Su Y, Cheng T, Shi C. A review of NIR dyes in cancer targeting and imaging. *Biomaterials* 2011; **32**: 7127–38.
28 Zhao T, Harada H, Teramura Y *et al.* A novel strategy to tag matrix metalloproteinases-positive cells for *in vivo* imaging of invasive and metastatic activity of tumor cells. *J Control Release* 2010; **144**: 109–14.
29 Myochin T, Hanaoka K, Komatsu T, Terai T, Nagano T. Design strategy for a near-infrared fluorescence probe for matrix metalloproteinase utilizing highly cell permeable boron dipyrromethene. *J Am Chem Soc* 2012; **134**: 13730–7.
30 Williams KC, Coppolino MG. Phosphorylation of membrane type 1-matrix metalloproteinase (MT1-MMP) and its vesicle-associated membrane protein 7 (VAMP7)-dependent trafficking facilitate cell invasion and migration. *J Biol Chem* 2011; **286**: 43405–16.
31 McCann TE, Kosaka N, Choyke PL, Kobayashi H. The use of fluorescent proteins for developing cancer-specific target imaging probes. *Methods Mol Biol* 2012; **872**: 191–204.
32 Licha K. Contrast agents for optical imaging. *Top Curr Chem* 2002; **222**: 1–29.
33 Tromberg BJ, Cerussi A, Shah N *et al.* Imaging in breast cancer: diffuse optics in breast cancer: detecting tumors in pre-menopausal women and monitoring neoadjuvant chemotherapy. *Breast Cancer Res* 2005; **7**: 279–85.
34 Polom K, Murawa D, Rho YS, Nowaczyk P, Hunerbein M, Murawa P. Current trends and emerging future of indocyanine green usage in surgery and oncology: a literature review. *Cancer* 2011; **117**: 4812–22.
35 Gioux S, Choi HS, Frangioni JV. Image-guided surgery using invisible near-infrared light: fundamentals of clinical translation. *Mol Imaging* 2010; **9**: 237–55.

Supporting Information

Additional supporting information may be found in the online version of this article:

Fig. S1. Western blotting analysis of the membrane type-1 matrix metalloproteinase (MT1-MMP) specific binding affinity of anti-MT1-MMP mAb used as a ligand of MT1-hIC7L.

Fig. S2. Flow cytometric analysis of MT1-hIC7L and anti-MT1-MMP antibody binding to membrane type-1 matrix metalloproteinase (MT1-MMP)-expressing cells.

Fig. S3. Western blotting and immunohistochemical analysis of the membrane type-1 matrix metalloproteinase (MT1-MMP) expression levels in C6 and MCF-7 xenografted tumor tissues.

Fig. S4. Uptake of MT1-hIC7L by HT1080 human fibroblastoma cells.

Data S1. Methods for western blotting flow cytometry, immunohistochemistry and cellular uptake of MT1-hIC7L.